Template-Directed One- and Two-Dimensional Copper(II) Diphosphonates: Structures and Characterizations of $(NH_4)_2Cu_3(hedp)_2(H_2O)_4$, $[NH_3(CH_2)_4NH_3]Cu_3(hedp)_2\cdot 2H_2O$, and $[NH_2(C_2H_4)_2NH_2]Cu_3(hedp)_2$ (hedp = 1-Hydroxyethylidenediphosphonate)

Li-Min Zheng,* Hui-Hua Song, Chun-Ying Duan, and Xin-Quan Xin

State Key Laboratory of Coordination Chemistry, Coordination Chemistry Institute, Nanjing University, Nanjing 210093, People's Republic of China

Received May 4, 1999

Three new copper(II) diphosphonates, $(NH_4)_2Cu_3(hedp)_2(H_2O)_4$ (**1**), $[NH_3(CH_2)_4NH_3]Cu_3(hedp)_2\cdot 2H_2O$ (**2**), and $[NH_2(C_2H_4)_2NH_2]Cu_3(hedp)_2$ (**3**), where hedp = 1-hydroxyethylidenediphosphonate, have been synthesized and characterized by single-crystal structural analysis. Crystal data: **1**, monoclinic, $P2_1/n$, $a = 6.2137(13)$ Å, $b = 14.747(2)$ Å, $c = 11.1802(12)$ Å, $\beta = 105.83(2)°$, $Z = 2$; **2**, triclinic, $P\bar{1}$, $a = 7.4840(12)$ Å, $b = 8.032(3)$ Å, $c = 10.007(2)$ Å, $\alpha = 111.68(2)°$, $\beta = 96.188(14)°$, $\gamma = 96.97(2)°$, $Z = 1$; **3**, triclinic, $P\bar{1}$, $a = 7.0155(6)$ Å, $b = 8.0904(9)$ Å, $c = 9.2644(11)$ Å, $\alpha = 112.611(13)°$, $\beta = 90.819(8)°$, $\gamma = 92.824(7)°$, $Z = 1$. The compound **1** is composed of infinite chains with a ladder-type motif. The compounds **2** and **3** adopt a two-dimensional layer structure which contains four- and eight-membered rings assembled from vertex-sharing $\{CuO_4\}$ units and $\{CPO_3\}$ tetrahedra. The magnetic properties of **3** have been investigated.

Introduction

The chemistry of metal phosphonates has been the subject of investigations for a decade. The interest in this area grew primarily out of the similarity of phosphonates of group 4 and 14 elements to the inorganic phosphates and their potential applications in exchange, catalysis, and sensors.[1−3] Subsequent studies from several research groups have shown that the metal phosphonates usually adopt layered or pillared layered structures.[4−7] The organic part of the phosphonates plays a space-filling role and participates in the two- and three-dimensional frameworks by strong covalent linkages. Only in some cases, exceptions have been observed, with the metal phosphonates showing different structure types including porous structures.[8−11]

Among these studies, the metal diphosphonates are of particular interest. By using diphosphonic acids, pillared or cross-linked compounds could be created. A few diphosphonate compounds with new structure types have also been reported.[12−14] It is, however, still a challenge in some cases to predict the metal diphosphonates with desired structures. There are at least three factors which may influence the arrangement of metal diphosphonates: (1) The length of the R tether in $H_2O_3P-R-PO_3H_2$. By increasing the number of methylene groups in $H_2O_3P-(CH_2)_x-PO_3H_2$, Haushalter and Zubieta et al.[15] have synthesized one ($x = 1$), two ($x = 2$) and three ($x = 3$) dimensional compounds of vanadium diphosphonates. (2) The protonation of the phosphonate oxygens. As observed in the chain compounds $Cu[HO_3P(C_6H_4)_2PO_3H]$[16] and $[Sn(HO_3PCH_2PO_3H]\cdot H_2O$,[17] the protonation of the phosphonate oxygens may block the assembly of metal diphosphonates into higher dimensionalities. (3) The template effect. Employing $NH_2(CH_2)_nNH_2$ ($n = 2, 3, 4$) as templates, three Ni(II)−$CH_3C(OH)(PO_3)_2$ complexes with one-dimensional to zero-dimensional (dimeric or monomeric) structures have been obtained.[18] This effect has not been well documented especially for the transition metal ions other than vanadium.[19]

Our interest in searching for the transition metal diphosphonates with new structural types, based on the 1-hydroxyethylidenediphosphonate [$CH_3C(OH)(PO_3)_2$, hedp] ligand, arised from the versatile coordination abilities of hedp in reacting with the metal ions (Scheme 1).

* To whom correspondence should be addressed. E-mail: lmzheng@netra.nju.edu.cn. Fax: +86-25-3314502.

(1) Zhang, B.; Clearfield, A. *J. Am. Chem. Soc.* **1997**, *119*, 2751.
(2) Alberti, G.; Constantino, U.; Casciola, M.; Vivani, R. *Adv. Mater*. **1996**, *8*, 291.
(3) Snover, J. L.; Byrd, H.; Suponeva, E. P.; Vicenzi, E.; Thompson, M. E. *Chem. Mater*. **1996**, *8*, 1490.
(4) Cao, G.; Hong, H.; Mallouk, T. E. *Acc. Chem. Res*. **1992**, *25*, 420.
(5) Poojary, M. D.; Hu, H. L.; Campbell, F. L., III; Clearfield, A. *Acta Crystallogr*. **1993**, *B49*, 996.
(6) Alberti, G. In *Comprehensive Supramolecular Chemistry*; Lehn, J. M., Ed.; Pergamon, Elsevier Science, Ltd.: Oxford, U.K., 1996; Vol. 7.
(7) Clearfield, A. In *Progress in Inorganic Chemistry*; Karlin, K. D., Ed.; John Wiley & Sons: New York, 1998; Vol. 47, pp 371−510.
(8) Le Bideau, J.; Payen, C.; Palvadeau, P.; Bujoli, B. *Inorg. Chem*. **1994**, *33*, 4885.
(9) Maeda, K.; Akimoto, J.; Kiyozumi, Y.; Mizukami, F. *Angew. Chem., Int. Ed. Engl*. **1995**, *34*, 1199.
(10) Poojary, M. D.; Grohol, D.; Clearfield, A. *Angew. Chem., Int. Ed. Engl*. **1995**, *34*, 1508.
(11) Bonavia, G.; Haushalter, R. C.; O'Connor, C. J.; Sangregorio, C.; Zubieta, J. *Chem. Commun*. **1998**, 2187.
(12) Lohse, D. L.; Sevov, S. C. *Angew. Chem., Int. Ed. Engl.* **1997**, *36*, 1619.
(13) Poojary, D. M.; Zhang, B.; Clearfield, A. *J. Am. Chem. Soc*. **1997**, *119*, 12550.
(14) Bonavia, G.; Haushalter, R. C.; O'Connor, C. J.; Zubieta, J. *Inorg. Chem*. **1996**, *25*, 5603.
(15) Soghomonian, V.; Chen, Q.; Haushalter, R. C.; Zubieta, J. *Angew. Chem., Int. Ed. Engl*. **1995**, *34*, 223.
(16) Poojary, D. M.; Zhang, B.; Bellinghausen, P.; Clearfield, A. *Inorg. Chem*. **1996**, *35*, 4942.
(17) Zapf, P. J.; Rose, D. J.; Haushalter, R. C.; Zubieta, J. *J. Solid State Chem*. **1996**, *125*, 182.
(18) Song, H. H.; Zheng, L. M.; Lin, C. H.; Wang, S. L.; Xin, X. Q.; Gao, S. *Chem. Mater*., in press.
(19) Soghomonian, V.; Diaz, R.; Haushalter, R. C.; O'Connor, C. J.; Zubieta, J. *Inorg. Chem*. **1995**, *34*, 4460 and references therein.

10.1021/ic990481r CCC: $18.00
Published on Web 10/02/1999

Scheme 1

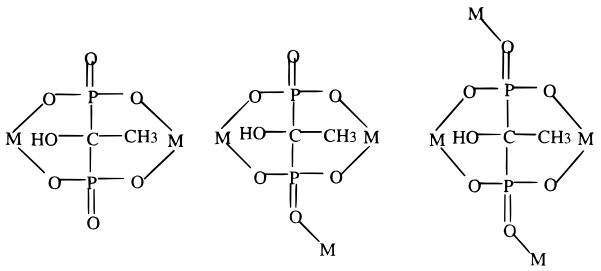

Analogous to the methylenediphosphonate, the short length of the R tether in hedp allows for the formation of stable M−O−P−C−P−O six-membered rings with the metal ions. In fact, hedp is more likely to behave as a bis(bidentate) bridging ligand using its four phosphonate oxygen atoms. The coordination of the remaining two oxygen atoms of $\{CPO_3\}$ moieties may lead to the construction of compounds with higher dimensionalities (Scheme 1). The additional $-CH_3$ and $-OH$ groups attached to the organic tether of hedp provide not only a steric hindrance but also a possible hydrophobic or hydrophilic environment which could be essential in the self-assembly of metal diphosphonates. Such flexible coordination capabilities of hedp have prompted us to carry out a systematic study on the metal−hedp compounds. The study has been especially focused on the template effects in directing structures. Our efforts along this line have resulted in the preparation of a mixed-valence copper(I/II) compound, $Na_2Cu_{15}(hedp)_6(OH)_2(H_2O)$, with porous structure[20] and several zero- to one-dimensional nickel−hedp compounds.[18] Herein we report the self-assembly of three new copper−hedp diphosphonates including ladderlike chain compound $(NH_4)_2Cu_3(hedp)_2(H_2O)_4$ (**1**) and layer compounds $[NH_3(CH_2)_4NH_3]Cu_3(hedp)_2{\cdot}2H_2O$ (**2**) and $[NH_2(C_2H_4)_2NH_2]$-$Cu_3(hedp)_2$ (**3**).

It is worth noting that only a few copper phosphonates have been structurally determined so far. They include one-dimensional chains of $Cu[HO_3P(C_6H_4)_2PO_3H]$,[16] two-dimensional layers of $Cu(RPO_3){\cdot}H_2O$ ($R = C_6H_5$, C_2H_5, CH_3)[21,22] and $Cu_3O(CH_3PO_3)_2{\cdot}2H_2O$,[8] and three-dimensional pillared layered or porous frameworks of β-$Cu(CH_3PO_3)$,[8] $Cu_2[(O_3PC_2H_4PO_3)(H_2O)_2]$,[13] $Cu_2[(O_3PC_3H_6PO_3)(H_2O)_2]{\cdot}H_2O$,[13] $Cu_2[(O_3PC_6H_4PO_3)(H_2O)_2]$,[16] and $Na_2Cu_{15}(hedp)_6(OH)_2(H_2O)$.[20]

Experimental Section

Materials and Methods. All the starting materials were reagent grade and used as purchased. The elemental analyses were performed on a PE 240C elemental analyzer. The infrared spectra were recorded on a IFS66V spectrometer with pressed KBr pellets. Variable-temperatue magnetic susceptibility data were obtained on a polycrystalline sample (81.3 mg for **3**) from 2 to 300 K in a magnetic field of 5 kG after zero-field cooling using a SQUID magnetometer. Diamagnetic corrections were estimated from Pascal's constants.[23] The temperature-independent paramagnetism (TIP) was estimated to be 60×10^{-6} cm^3 mol^{-1} for copper(II) mononuclear species.

Synthesis of $(NH_4)_2Cu_3(hedp)_2(H_2O)_4$, 1. A mixture of $Cu(NO_3)_2{\cdot}3H_2O$ (1 mmol, 0.2436 g), 50% $hedpH_4$ (1 cm^3), NH_4HF_2 (1 mmol, 0.0592 g), and H_2O (8 cm^3), adjusted by $NH_3{\cdot}H_2O$ to pH $\approx$ 3, was kept in a Teflon-lined autoclave at 140 °C for 2 d. After the mixture was slowly cooled to room temperature, blue needlelike crystals were collected as a monophasic material, judged by the powder X-ray diffraction pattern, which were further used for the structural determination and the physical property measurements. Anal. Found: C, 7.06; H, 3.37; N, 4.23. Calcd for $C_4H_{24}Cu_3N_2O_{18}P_4$: C, 6.83; H, 3.42; N, 3.99. IR (KBr, cm^{-1}): 3438m, 3034m (br), 1704w, 1679w, 1485m, 1455m, 1433m, 1421m, 1369w, 1158s, 1125s, 1085s, 1073s, 1038s, 997s, 953m, 900w, 827m, 784w, 672m, 590s, 505m, 460w, 421w. Compound **1** can also be obtained as a monophase following a similar reaction procedure but at different temperatures (110 and 180 °C) and using different amounts of $Cu(NO_3)_2{\cdot}3H_2O$ (2 and 3 mmol). A reduced amount of $Cu(NO_3)_2{\cdot}3H_2O$ (0.5 mmol) at 140 °C led to the formation of copper powder.

Synthesis of $[NH_3(CH_2)_4NH_3]Cu_3(hedp)_2{\cdot}2H_2O$, 2. The compound was prepared from a mixture of $Cu(NO_3)_2{\cdot}3H_2O$ (3 mmol, 0.7259 g), 50% $hedpH_4$ (1 cm^3), LiF (1 mmol, 0.0256 g), $H_2C_2O_4{\cdot}2H_2O$ (1 mmol, 0.1266 g), and H_2O (8 cm^3), adjusted by $NH_2(CH_2)_4NH_2$ to pH $\approx$ 3.5, in a Teflon-lined autoclave at 140 °C for 2 d. Blue crystals were produced as a single phase, judged by the powder X-ray pattern in comparison with the pattern deduced from single-crystal data. The product was further used for single-crystal structural determination and property measurements. Anal. Found: C, 13.29; H, 3.49; N, 3.89. Calcd for $C_8H_{26}Cu_3N_2O_{16}P_4$: C, 13.32; H, 3.61; N, 3.88. IR (KBr, cm^{-1}): 3573m, 3405m, 3169s (br), 1632m, 1602m, 1509m, 1471w, 1445w, 1380w, 1294w, 1142s, 1094vs, 1049vs, 1001s, 954s, 904w, 884w, 811m, 749w, 684m, 590s, 558m, 499m, 451m, 422m, 404w. Reactions under similar hydrothermal conditions except using smaller amounts of $Cu(NO_3)_2{\cdot}3H_2O$ (2, 1, and 0.5 mmol) promoted the formation of an unidentified phase or even copper powder.

Synthesis of $[NH_2(C_2H_4)_2NH_2]Cu_3(hedp)_2$, 3. The hydrothermal treatment of a mixture of $Cu(NO_3)_2{\cdot}3H_2O$ (1 mmol, 0.2478 g), 50% $hedpH_4$ (1 cm^3), piperazine (2 mmol, 0.3327 g), and H_2O (8 cm^3) (pH $\approx$ 3) in a Teflon-lined autoclave at 140 or 180 °C for 3 d resulted in the formation of compound **3** as a monophasic material. The dark blue crystals were used for single-crystal structural determination and property measurements. Anal. Found: C, 13.97; H, 2.99; N, 4.19. Calcd for $C_8H_{20}Cu_3N_2O_{14}P_4$: C, 14.07; H, 2.95; N, 4.10. IR (KBr, cm^{-1}): 3148m, 2767m (br), 1631m, 1486w, 1457m, 1167s, 1079s, 1039s, 994s, 955s, 901w, 818m, 677m, 625w, 589m, 579m, 556m, 506m, 448m, 424w. The compound was obtained similarly using 2 or 3 mmol of $Cu(NO_3)_2{\cdot}3H_2O$ at 180 or 140 °C. Compounds **1**−**3** can be obtained without the addition of fluorides and $H_2C_2O_4$ (for **2**), although with them more crystalline products can be obtained, which is possibly due to their complexing properties toward the metal atoms.

X-ray Crystallographic Analysis. Crystals with dimensions 0.80 × 0.40 × 0.40 mm for **1**, 0.25 × 0.25 × 0.10 mm for **2**, and 0.50 × 0.50 × 0.30 mm for **3** were selected for indexing and intensity data collection at 293(2) K on a Siemens P4 four-circle diffractometer with monochromated Mo Kα (λ = 0.710 73 Å) radiation. Cell constants and an orientation matrix for data collection were obtained from least-squares refinement of the setting angles of 66 randomly oriented reflections in the range $5.78 < \theta < 16.80$ for **1**, corresponding to a monoclinic cell. For **2**, a triclinic cell was determined by least-squares refinement of the θ angles of 34 reflections in the interval $6.8 < \theta < 12.32$. For **3**, a triclinic unit cell was determined from 31 indexed reflections in the range $8.77 < \theta < 13.83$. As a check on crystal and instrument stability, 3 representative reflections were measured every 100 for **1**−**3**, and decays of 12.47 and 4.83 were observed for **1** and **3**, respectively. Intensity data were collected using the $\theta-2\theta$ scan mode with a variable scan speed of 5.0−50.0 deg min^{-1} in ω. Number of measured and observed reflections [$I > 2\sigma(I)$]: 2434, 1735 (R_{int} = 0.0465) for **1**; 2017, 1865 (R_{int} = 0.0362) for **2**; 2648, 2047 (R_{int} = 0.0189) for **3**. The data were corrected for Lorentz-polarization effects during data reduction using XSCANS.[24] Empirical absorption corrections based on ψ-scan measurements were applied ($T_{min,max}$: 0.0786, 0.2319 for **1**; 0.3397, 0.4738 for **2**; 0.3150, 0.5098 for **3**). An extinction correction was applied for **3**, with the extinction coefficient 0.051(4).

The structures were solved by direct methods and refined on F^2 by full-matrix least squares using SHELXTL.[25] All the non-hydrogen atoms

(20) Zheng, L. M.; Duan, C. Y.; Ye, X. R.; Zhang, L. Y.; Wang, C.; Xin, X. Q. *J. Chem. Soc., Dalton Trans.* **1998**, 905.
(21) Zhang, Y.; Clearfield, A. *Inorg. Chem.* **1992**, *31*, 2821.
(22) Le Bideau, J.; Bujoli, B.; Jouanneaux, A.; Payen, C.; Palvadeau, P.; Rouxel, J. *Inorg. Chem.* **1993**, *32*, 4617.
(23) Kahn, O. *Molecular Magnetism*; VCH Publishers: New York, 1993.
(24) XSCANS (version 2.1), Siemens Analytical X-ray Instruments, Madison, WI, 1994.

Table 1. Crystallographic Data for **1**−**3**

compound	**1**	**2**	**3**
empirical formula	$C_4H_{24}Cu_3N_2O_{18}P_4$	$C_8H_{26}Cu_3N_2O_{16}P_4$	$C_8H_{20}Cu_3N_2O_{14}P_4$
fw	702.75	720.80	682.76
space group	$P2_1/n$	$P\bar{1}$	$P\bar{1}$
a, Å	6.2137(13)	7.4840(12)	7.0155(6)
b, Å	14.747(2)	8.032(3)	8.0904(9)
c, Å	11.1802(12)	10.007(2)	9.2644(11)
α, deg		111.68(2)	112.611(13)
β, deg	105.83(2)	96.188(14)	90.819(8)
γ, deg		96.97(2)	92.824(7)
V, Å^3	985.6(3)	547.3(3)	484.51(9)
Z	2	1	1
D_c, g cm^{-3}	2.368	2.187	2.340
μ(Mo Kα), cm^{-1}	36.25	32.61	36.69
R_1, wR_2 [$I > 2\sigma(I)$][a]	0.0435, 0.1166	0.0494, 0.1362	0.0306, 0.0869
R_1, wR_2 (all data)[a]	0.0439, 0.1172	0.0588, 0.1452	0.0318, 0.0878

[a] $R_1 = \sum||F_o| - |F_c||/\Sigma|F_o|$. w$R_2 = [\sum w(F_o^2 - F_c^2)^2/\Sigma w(F_o^2)^2]^{1/2}$.

Table 2. Selected Bond Lengths (Å) and Angles (deg) for **1**[a]

Cu(1)−O(1)	1.953(2), 2×	Cu(1)−O(4)	1.973(2), 2×
Cu(2)−O(5)	1.931(3)	Cu(2)−O(6B)	1.906(3)
Cu(2)−O(2)	1.963(3)	Cu(2)−O(1W)	2.273(3)
Cu(2)−O(2W)	1.990(3)	P(1)−O(1)	1.535(3)
P(1)−O(3)	1.506(3)	P(1)−O(2)	1.535(3)
P(2)−O(4)	1.537(3)	P(1)−O(2)	1.535(3)
P(2)−O(6)	1.509(3)		
O(1A)−Cu(1)−O(1)	180.0, 2×	O(1)−Cu(1)−O(4)	90.51(12), 2×
O(1)−Cu(1)−O(4A)	89.49(12), 2×	O(5)−Cu(2)−O(2)	93.64(11)
O(6B)−Cu(2)−O(5)	158.55(13)	O(6B)−Cu(2)−O(2)	92.53(11)
O(6B)−Cu(2)−O(2W)	84.14(13)	O(5)−Cu(2)−O(2W)	87.52(13)
O(2)−Cu(2)−O(2W)	173.37(13)	O(6B)−Cu(2)−O(1W)	105.49(13)
O(5)−Cu(2)−O(1W)	94.70	O(2)−Cu(2)−O(1W)	92.82(12)
O(2W)−Cu(2)−O(1W)	93.58(13)	P(1)−O(1)−Cu(1)	121.9(2)
P(1)−O(2)−Cu(2)	132.3(2)	P(2)−O(4)−Cu(1)	120.0(2)
P(2)−O(5)−Cu(2)	125.6(2)	P(2)−O(6)−Cu(2C)	143.4(2)

[a] Symmetry code: A, $-x - 1$, $-y + 1$, $-z + 1$; B, $x - 1$, y, z; C, $x + 1$, y, z.

were refined anisotropically, except the C atoms of $NH_3(CH_2)_4NH_3^{2+}$ cations in **2**, which are disordered. For **2**, the hydrogen atoms of the methyl and hydroxy groups were placed in calculated positions (C−H = 0.96 Å) and allowed to ride on their respective parent atoms. The H atoms in H_2O were found from the Fourier-difference map. All the hydrogen atoms were assigned fixed isotropic thermal parameters 1.5 times the equivalent isotropic U of the atoms to which they are attached. For **1** and **3**, the hydrogen atoms were found from the Fourier difference maps and refined isotropically. The contributions of the hydrogen atoms were included in the structure-factor calculations. In the final Fourier-difference maps the deepest hole and the highest peak were −1.380 and 1.046 e/Å^3 for **1**, −0.914 and 1.399 e/Å^3 for **2**, and −1.194 and 0.552 e/Å^3 for **3**, respectively.

All computations were carried out on a PC-586 computer using the SHELXTL package. Analytical expressions of neutral-atom scattering factors and anomalous dispersion corrections were incorporated. Selected crystallographic data and structure determination parameters for **1**−**3** are given in Table 1.

Results and Discussions

Crystal Structure of $(NH_4)_2Cu_3(hedp)_2(H_2O)_4$, 1. The selected bond lengths and angles for **1** are listed in Table 2. The structure of **1** consists of infinite anionic copper(II)−hedp chains with a ladder-type motif, which are charge-balanced by NH_4^+ cations. The chain is constructed from the symmetric $Cu_3(hedp)_2(H_2O)_4^{2-}$ building blocks (Figure 1). The Cu(1) atom is in a planar environment with the four oxygen atoms from centrosymmetrically related hedp groups. The average Cu(1)−O bond length is 1.963(3) Å. The Cu(2) atom, however, bears a distorted square pyramidal coordination geometry. The basel plane is defined by O(2), O(5), O(6B), and O(2w) with the largest deviation of 0.1203 Å at O(2w). The Cu(2) atom is pulled out of this plane by 0.2212 Å. The apical position is occupied by O(1w) of a water molecule. The Cu(2)−O(1w) distance [2.273(3) Å] is longer than the other Cu(2)−O distances [1.906(3)−1.990(3) Å]. The hedp group bridges the Cu(1) and Cu(2) atoms through the bis(bidentate) mode, using four oxygen atoms from its two {CPO_3} moieties. One of the remaining two oxygen atoms, O(6), is further linked to the Cu(2) atom in the neighboring $Cu_3(hedp)_2(H_2O)_4^{2-}$ trimer units. The other oxygen

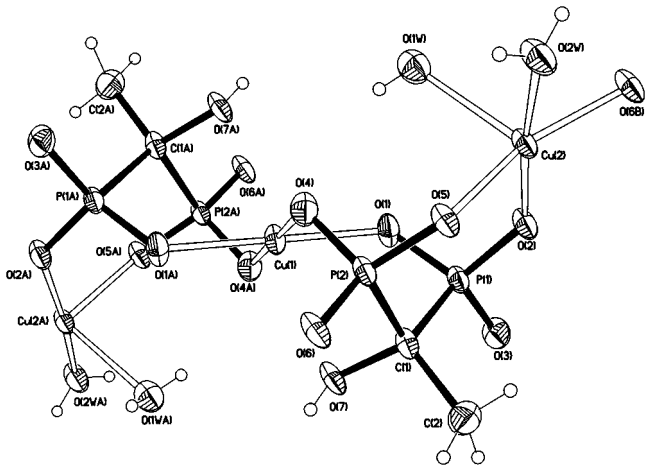

Figure 1. Trimer unit in **1** with the atomic labeling scheme (50% probability).

(25) SHELXTL (version 5.0) Reference Manual, Siemens Industrial Automation, Analytical Instrumentation, Madison, WI, 1995.

Table 3. Selected Bond Lengths (Å) and Angles (deg) for **2**[a]

Cu(1)−O(1)	1.935(4), 2×	Cu(1)−O(4)	1.961(4), 2×
Cu(2)−O(2)	1.930(3)	Cu(2)−O(6B)	1.926(3)
Cu(2)−O(3C)	1.949(4)	Cu(2)−O(5)	2.008(4)
P(1)−O(1)	1.521(3)	P(1)−O(3)	1.535(4)
P(1)−O(2)	1.518(4)	P(2)−O(4)	1.517(4)
P(2)−O(5)	1.544(4)	P(2)−O(6)	1.534(3)
O(1A)−Cu(1)−O(1)	180.0, 2×	O(1)−Cu(1)−O(4)	94.70(14), 2×
O(1)−Cu(1)−O(4A)	85.30(14), 2×	O(2)−Cu(2)−O(5)	88.83(14)
O(6B)−Cu(2)−O(2)	173.0(2)	O(6B)−Cu(2)−O(3C)	89.00(14)
O(2)−Cu(2)−O(3C)	91.56(14)	O(6B)−Cu(2)−O(5)	93.1(2)
O(3C)−Cu(2)−O(5)	159.14(14)	P(2)−O(4)−Cu(1)	135.5(2)
P(1)−O(1)−Cu(1)	129.4(2)	P(1)−O(3)−Cu(2C)	120.4(2)
P(1)−O(2)−Cu(2)	119.3(2)	P(2)−O(5)−Cu(2)	118.6(2)
P(2)−O(6)−Cu(2B)	130.8(2)		

[a] Symmetry code: A, $-x+1, -y, -z+1$; B, $-x+1, -y-1, -z$; C, $-x+1, -y, -z$.

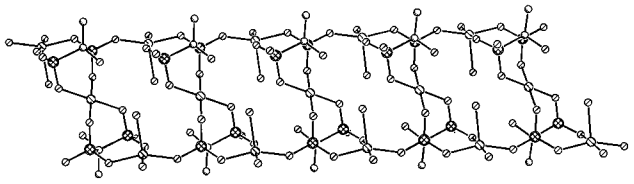

Figure 2. A fragment of the chain in **1** showing the ladder-type motif. All H atoms are omitted.

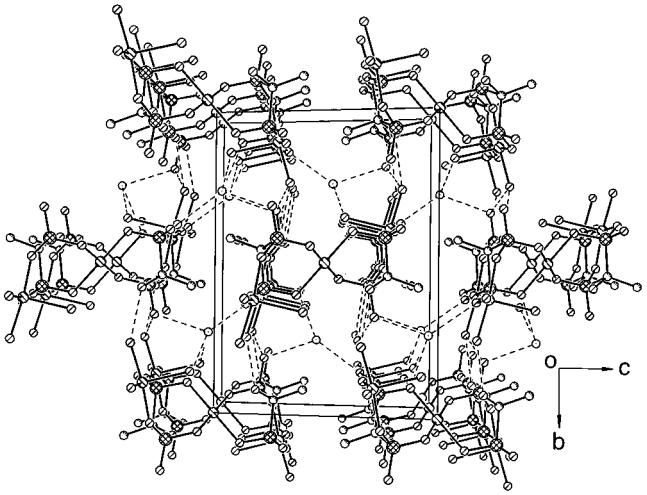

Figure 3. Structure of **1** packed along the *a*-axis. All the H atoms are omitted.

atom, O(3), remains to be pendant [P(1)═O(3) = 1.506(3) Å]. Therefore, the side pieces of the ladder chains are formed by the {Cu(2)O_5} tetragonal pyramidals and the {CPO_3} tetrahedra, whereas the rungs of the ladder are formed by the {Cu(1)O_4} planes (Figure 2).

Between the chains, there exists extensive hydrogen bonding. The lattice is further stabilized by NH_4^+ cations through hydrogen bonding to the lattice water, the hydroxy groups, or pendant O(3) atoms. The four shortest N···O contact distances are 2.810(6), 2.834(5), 2.850(5), and 2.913(5) Å for N···O1w^{i}, N···O3^{ii}, N···O5^{iii}, and N···O4^{iv} (symmetry code: i, $-x-3/2, y-1/2, -z+3/2$; ii, $x+1, y, z+1$; iii, $-x-1, -y+1, -z+1$; iv, $-x-1/2, y-1/2, -z+3/2$), respectively. Figure 3 exhibits the crystal packing arrangement in the [100] projection.

Crystal Structure of $[NH_3(CH_2)_4NH_3]Cu_3(hedp)_2\cdot 2H_2O$, 2. The fundamental building unit of **2** is a linear trimer of $Cu_3(hedp)_2^{2-}$, shown in Figure 4 with the atomic labeling scheme. The selected bond lengths and angles for **2** are summarized in Table 3. In the $Cu_3(hedp)_2^{2-}$ trimer, two types of copper(II) atoms are distinguished, both of which are four-

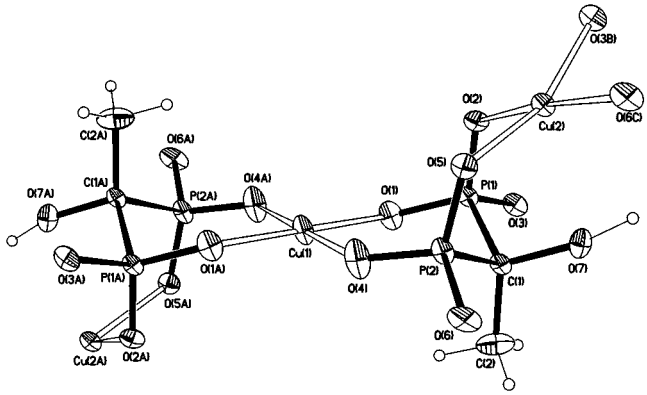

Figure 4. Trimer unit in **2** with the atomic labeling scheme (50% probability).

coordinated. The Cu(1) atom, sitting in an inversion center, has a planar geometry with the four-coordinated oxygen atoms from two equivalent $hedp^{4-}$ ligands. The Cu(1)−O distances are 1.935(4) and 1.961(4) Å. The Cu(2) atom is in a distorted tetrahedral environment with the four oxygen atoms from three different hedp groups. The Cu(2)−O(5) bond length [2.008(4) Å] is distinctly longer than that of Cu(2)−O(2) [1.930(3) Å]. The average Cu−O distance [1.951(4) Å] can be compared with those in $Na_2Cu_{15}(hedp)_6(OH)_2(H_2O)$ [mean Cu−O = 1.960(8) Å].[20] The trimer contains two centrosymmetrically related $hedp^{4-}$ ligands. Each hedp is multidentate, and bridges Cu(1) and Cu(2) atoms in a bisbidentate mode in one trimer. The remaining two oxygen atoms of {CPO_3} moieties are connected to Cu(2) atoms in the neighboring two trimers. Therefore, a two-dimensional anionic layer is constructed which contains four- and eight-membered rings assembled from vertex-sharing {CuO_4} units and {CPO_3} tetrahedra (Figure 5). Between the layers, there exist water molecules and diprotonated $NH_3(CH_2)_4NH_3^{2+}$ cations, thus forming alternately arranged anionic−cationic sheets as shown in Figure 6. The sheets are stacked along the *a*-axis, forming one-dimensional channels in the [100] direction where the diprotonated $NH_3(CH_2)_4NH_3^{2+}$ cations and water molecules reside. The $NH_3(CH_2)_4NH_3^{2+}$ cations are disordered. Extensive hydrogen bonding is found between the $NH_3(CH_2)_4NH_3^{2+}$ cations and the anionic layers or water molecules: N(1)···O(3)^{i} = 2.789(8) Å, N(1)···O(3)^{ii} = 3.305(6) Å, N(1)···O(2)^{iii} = 2.844(7) Å, N(1)···O(7)^{ii} = 3.048(9) Å, N(1)···O(1w)^{iv} = 2.885(10) Å, N(2)···O(1) = 2.998(14) Å, N(2)···O(1)^{iii} = 3.361(13) Å, N(2)···O(6)^{iv} = 3.142(15) Å, N(2)···O(4)^{iv} = 2.845(17) Å, N(2)···O(4)^{v} = 2.863(17) Å (symmetry code: i, $-x, -y+1, -z+1$; ii, $x, y+1, z+1$; iii, $-x+1, -y+1, -z+1$; iv, $x, y+1, z$; v, $-x+1, -y, -z+1$).

Table 4. Selected Bond Lengths (Å) and Angles (deg) for **3**[a]

Cu(1)−O(1)	1.931(2), 2×	Cu(1)−O(4)	1.948(2), 2×
Cu(2)−O(3B)	1.919(2)	Cu(2)−O(2)	1.945(2)
Cu(2)−O(6B)	1.967(2)	Cu(2)−O(5)	1.983(2)
P(1)−O(1)	1.544(2)	P(1)−O(3)	1.512(2)
P(1)−O(2)	1.520(2)	P(2)−O(4)	1.522(2)
P(2)−O(5)	1.539(2)	P(2)−O(6)	1.533(2)
O(1)−Cu(1)−O(1A)	180.0, 2×	O(1)−Cu(1)−O(4)	92.01(9), 2×
O(1)−Cu(1)−O(4A)	87.99(9), 2×	O(2)−Cu(2)−O(5)	89.21(8)
O(3B)−Cu(2)−O(2)	91.68(8)	O(3B)−Cu(2)−O(6C)	88.16(8)
O(2)−Cu(2)−O(6C)	175.75(8)	O(3B)−Cu(2)−O(5)	167.49(8)
O(6C)−Cu(2)−O(5)	91.87(8)	P(1)−O(1)−Cu(1)	116.90(11)
P(2)−O(4)−Cu(1)	125.00(12)	P(1)−O(2)−Cu(2)	117.27(11)
P(2)−O(5)−Cu(2)	118.67(11)	P(1)−O(3)−Cu(2B)	126.40(12)
P(2)−O(6)−Cu(2C)	128.17(12)		

[a] Symmetry code: A, $-x+2, -y+1, -z+2$; B, $-x+2, -y+1, -z+1$; C, $-x+2, -y, -z+1$.

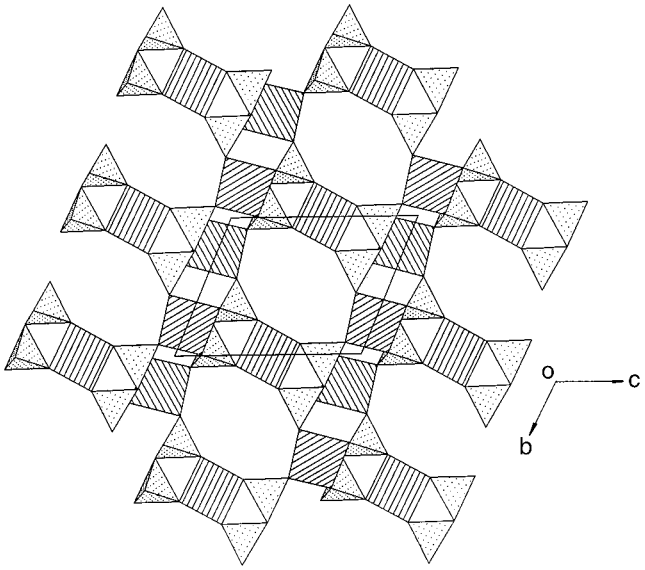

Figure 5. Polyhedral representation of structure **2** packed along the [100] direction. All the H, C2, and O7 atoms and $[NH_3(CH_2)_4NH_3]^{2+}$ cations are omitted for clarity.

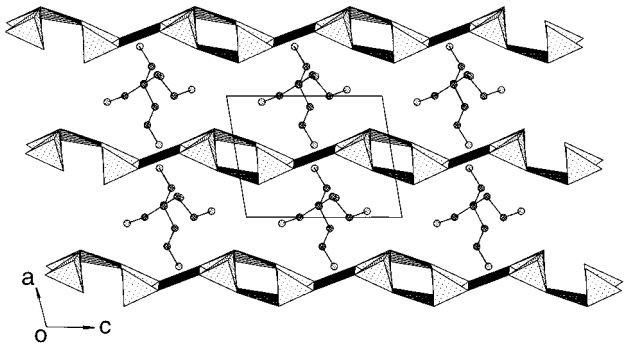

Figure 6. Polyhedral representation of structure **2** packed along the [010] direction. All the H, C2, and O7 atoms are omitted for clarity.

Crystal Structure of $[NH_2(C_2H_4)_2NH_2]Cu_3(hedp)_2$, 3. The structure of **3** is very similar to that of **2**, except that the cell volume of **3** is slightly reduced. It is two-dimensional with the anionic layers built up from the vertex-sharing $\{CuO_4\}$ units and $\{CPO_3\}$ tetrahedra. The charge-compensating cations, however, are diprotonated piperazine which lie between the layers (Figure 7). These cations are ordered and stabilize the lattice by forming hydrogen bonds with the oxygen atoms in the neighboring layers. The three shortest N···O distances are 2.727(4), 2.937(3), and 2.841(4) Å for N(1)···O(1), N(1)···O(3), and N(1)···O(6)^{i} (symmetry code: i, $x, y+1, z$), respectively. The selected bond lengths and angles for **3** are listed in Table 4.

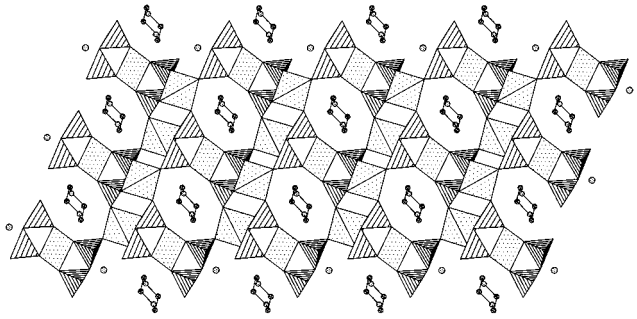

Figure 7. Polyhedral representation of structure **3** packed along the [100] direction. All the H, C2, and O7 atoms are omitted for clarity.

The structures of **1**−**3** are strikingly distinguished from the other copper phosphonates previously reported. In $Cu(O_3PR)\cdot H_2O$ ($R = CH_3, C_2H_5, C_6H_5$) and $Cu_2[(O_3PC_6H_4PO_3)(H_2O)]$, the purely inorganic layers of Cu−O_3P are separated or cross-linked by the organic groups. The ladder-like chain in **1** and the sheet in **2** and **3**, however, are built up from both inorganic and organic units. A similar phenomenon has been observed in vanadium methylenediphosphonates ($O_3PCH_2PO_3$) such as, for instance, $(VO)_2(O_3PCH_2PO_3)\cdot 4H_2O$[26] and $[V(HO_3PCH_2PO_3)(H_2O)]$.[27]

Template Effect in Directing the Crystal Structures. By changing the templates from NH_3 to 1,4-butylenediamine and piperazine, with the same bridging ligand and metal salt, we have succeeded in synthesizing two types of copper(II)−hedp complexes. Compound **1** has a ladder-like chain structure, while compounds **2** and **3** have two-dimensional layer structures. In all three compounds, there exists an analogous building unit of $Cu^{II}_3(hedp)_2$ trimer. In this trimer, each hedp group bridges the Cu(1) and Cu(2) atoms in a bis(bidentate) mode. The remaining four phosphonate oxygens in the trimer, which could be accordingly viewed as a potential tetradentate "ligand", coordinates to the Cu(2) atoms in the neighboring trimer units, thus forming two-dimensional layered structures of **2** and **3**. The development of such a layer is blocked in **1**, which shows one-dimensional chain structure with the coordination of the Cu(2) atom terminated by two water molecules. Therefore, the Cu(2) has a square pyramidal environment in **1**, whereas it has a distorted tetrahedral arrangement in **2** and **3**. The pronounced

(26) Huan, G.; Johnson, J. W.; Jacobson, A. J.; Merola, J. S. *J. Solid State Chem.* **1990**, *89*, 220.
(27) Bonavia, G.; Haushalter, R. C.; O'Connor, C. J.; Zubieta, J. *Inorg. Chem.* **1996**, *35*, 5603.

structural differences in **1**−**3** can be related to the templates employed in the hydrothermal reactions, because the preparations of the three compounds were conducted under similar experimental conditions. Although the other factors such as the molar ratio of the starting materials, temperature, pH, etc. can be important to the final product, the failure of our attempts, by using NH_3 as template, to synthesize a similar layered compound under various experimental conditions has revealed that the templates play a key role in directing the structures of **1**−**3**. Actually, these templates serve as the charge-compensating counterions of the polymeric anions in **1**−**3**. The cations $NH_3(CH_2)_4NH_3^{2+}$ and $NH_2(C_2H_4)_2NH_2^{2+}$ with larger size favor packing with a two-dimensional anionic layer, whereas the NH_4^+ with a smaller size directs the formation of an anionic chain.

It is recalled that a molar ratio of 3:2 for Cu(II):hedp is also observed in the three-dimensional mixed-valence compound $Na_2Cu^I_6Cu^{II}_9(hedp)_6(OH)_2(H_2O)$.[20] In this compound, each hedp group bridges the Cu(1) and Cu(2) atoms in a bis(bidentate) manner identical to those in structures **1**−**3**. It is, however, the incorporation of sodium ions which coordinate to the phosphonate oxygens through edge-sharing with the $\{CuO_4\}$ planes that directs the formation of a three-dimensional porous structure. These results demonstrate that one-, two-, and three-dimensional metal complexes of hedp are reachable by a suitable choice of inorganic species or organic templates. New structural types could be expected through the introduction of matched templates or an appropriate second metal ion, which may further bring interesting physical properties.

Infrared Spectra and Magnetic Properties. The infrared spectra of **1**−**3** exhibit a series of bands in the 1000−1200 cm^{-1} range, corresponding to the phosphonate PO_3 group vibrations. The broad band appearing around 3200 cm^{-1} can be due to O−H stretching of hydrogen-bonded hydroxyl groups including water molecules and the α-hydroxy group.[28]

The temperature-dependent magnetic susceptibility for **3** was measured in the temperature range from 300 to 2 K. Figure 8 shows the $\chi_m T$ vs T plot of the molecule. At 300 K, the magnetic moment (μ_{eff}) per copper(II) atom of **3**, determined from the equation $\mu_{eff} = 2.828(\chi_m T)^{1/2}$, is 1.97 μ_B, which is close to the value expected for an isolated system of $S = 1/2$ ($\mu_{eff} = 1.90$ μ_B for $g = 2.2$). Upon cooling, $\chi_m T$ decreases and reaches a minimum of 0.75 cm^3 K mol^{-1} at 34 K, indicating an antiferromagnetic interaction which is attributed to the exchange

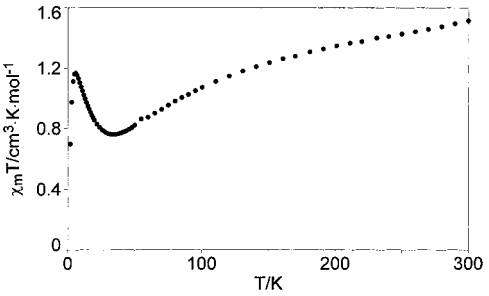

Figure 8. $\chi_m T$ vs T for **3**.

couplings between Cu(II) centers through O−P−O bridges. The increase of $\chi_m T$ below 34 K could be due to a large contribution from a paramagnetic impurity or due to a substantial contribution from ferromagnetic coupling. As the highly crystalline specimens with satisfactory analytical data and XRD pattern were used for the magnetic measurements, the contribution of the impurities should be ruled out. Ferromagnetic coupling could be dominant at low temperature. However, the origin of such a ferromagnetic exchange is not clear to us right now.

Conclusions

Three new copper(II) diphosphonates which contain a similar $Cu^{II}_3(hedp)_2$ trimer unit are described in this paper. Compound **1**, with a smaller template cation, NH_4^+, bears a ladder-like chain structure. Compounds **2** and **3**, with a larger template cation, $NH_3(CH_2)_4NH_3^{2+}$ or $NH_2(C_2H_4)_2NH_2^{2+}$, show two-dimensional layered structures. The distinct differences in the structural features between the chain compound **1** and the layer compounds **2** and **3** are mainly attributed to the template effects during the hydrothermal reactions. These templates, acting as charge-compensating counterions, play an important role in the crystal packing with the polymeric anionic chains or networks.

Acknowledgment. The support of the National Natural Science Foundation of China, Natural Science Foundation of Jiangsu province, and Analysis Center of Nanjing University are acknowledged. We are also indebted to Mr. Yong-Jiang Liu for single-crystal X-ray data collection and Professor K. H. Lii for the magnetic susceptibility measurements.

Supporting Information Available: Figures of infrared spectra and powder XRD patterns, and X-ray crystallographic files, in CIF format, for the three compounds. This material is available free of charge via the Internet at http://pubs.acs.org.

IC990481R

(28) Nash, K. L.; Rogers, R. D.; Ferraro, J.; Zhang, J. *Inorg. Chim. Acta* **1998**, *269*, 211.